Physics of Semiconductors. Semiconductors

UDC 538.945.9

EDN NFNKXG
https://www.doi.org/10.33910/2687-153X-2022-3-2-86-99

Electronic defects in lattices of YBa_2Cu_3O7 and $La_{2-x}Sr_xCuO_4$

A. V. Marchenko[1], P. P. Seregin✉[1], V. S. Kiselev[1]

[1] Herzen State Pedagogical University of Russia, 48 Moika Emb., Saint Petersburg 191186, Russia

Authors

Alla V. Marchenko, ORCID: 0000-0002-9292-2541, e-mail: al7140@rambler.ru

Pavel P. Seregin, ORCID: 0000-0001-5004-2047, e-mail: ppseregin@mail.ru

Valentin S. Kiselev, e-mail: kiselev.valentin@gmail.com

For citation: Marchenko, A. V., Seregin, P. P., Kiselev, V. S. (2022) Electronic defects in lattices of $YBa_2Cu_3O_7$ and $La_{2-x}Sr_xCuO_4$. *Physics of Complex Systems*, 3 (2), 86–99. https://www.doi.org/10.33910/2687-153X-2022-3-2-86-99. EDN NFNKXG

Received 28 February 2022; reviewed 28 March 2022; accepted 28 March 2022.

Funding: The study did not receive any external funding.

Abstract. Using emission Mössbauer spectroscopy data for the ^{67}Zn isotope and nuclear quadrupole resonance data for the ^{17}O isotope, as well as calculations of the lattice electric field gradient, the effective charges of all atoms in superconducting copper metal oxide $YBa_2Cu_3O_7$ and $La_{2-x}Sr_xCuO_4$ crystal lattices were determined. The effective charges of metal atoms and most oxygen atoms correspond to their standard oxidation states (Y^{3+}, La^{3+}, Ba^{2+}, Sr^{2+}, Cu^{2+} and O^{2-}). However, the atoms of chain oxygen (in $YBa_2Cu_3O_7$) and planar oxygen (in $YBa_2Cu_3O_7$ and $La_{2-x}Sr_xCuO_4$) show a reduced charge, which is explained by the localisation of holes in the corresponding sublattices.

Keywords: Mössbauer spectroscopy, nuclear quadrupole resonance, electric field gradient tensor, atomic charges, high-temperature superconductors

Introduction

The discovery of the high-temperature superconductivity phenomenon in copper metal oxides (Bednorz, Muller 1986) resulted in a large number of studies of nuclear quadrupole interaction (NQI) in typical materials of this kind—$YBa_2Cu_3O_{7-x}$ and $La_{2-x}Sr_xCuO_4$—through nuclear quadrupole resonance (NQR) method with probe nuclei ^{17}O (Ishida et al. 1991; Takigawa et al. 1989), ^{63}Cu (Ohsugi et al. 1994; Pennington et al. 1989), ^{137}Ba (Shore et al. 1992), ^{139}La (Ohsugi 1995), as well as through absorption Mössbauer spectroscopy (MS) with probe nuclei ^{57}Fe, ^{119}Sn, ^{151}Eu, ^{155}Gd, ^{161}Dy, ^{166}Er, ^{169}Tm, ^{170}Yb (Masterov et al. 1995) and emission MS with probe nuclei $^{67}Cu(^{67}Zn)$ and $^{67}Ga(^{67}Zn)$ (Marchenko et al. 2018a; 2018b; Terukov et al. 2018). NQI tensor parameters (the quadrupole interaction constant and the asymmetry parameter) provide information on the spatial distribution of electronic defects in various sublattices within high-temperature superconductors (HTSC). This information makes it possible to determine the effective charges of their atoms, which, in turn, naturally limits the number of models that should be used in quantum mechanical calculations of HTSC electronic properties. A reliable method for finding the effective charges of atoms is to compare the calculated and the experimental parameters of the NQI tensor.

In crystal lattices with high chemical bond ionicity, which includes copper metal oxides $YBa_2Cu_3O_{7-x}$ and $La_{2-x}Sr_xCuO_4$, two sources of the electric field gradient (EFG) on probe nuclei can be distinguished: crystal lattice ions (lattice EFG) and nonspherical valence shells of the probe atoms (valence EFG). The total EFG on the probe nucleus is determined by the parameters (Marchenko et al. 2018a; 2018b)

$$U_{zz} = (1-\gamma)V_{zz} + (1-R_0)W_{zz}, \quad (1)$$

$$\eta = \frac{(1-\gamma)V_{zz}\eta_{lat} + (1-R_0)W_{zz}\eta_{val}}{U_{zz}}, \quad (2)$$

$$\eta = \frac{U_{xx}-U_{yy}}{U_{zz}}, \eta_{cr} = \frac{V_{xx}-V_{yy}}{V_{zz}}, \eta_{val} = \frac{W_{xx}-W_{yy}}{W_{zz}}, \quad (3)$$

where U_{ii}, V_{ii}, and W_{ii} are the components of the diagonalised total, lattice and valence EFG tensors, U_{zz}, V_{zz}, and W_{zz} are the principal components of these tensors, η, η_{lat}, η_{val} are the asymmetry parameters of these tensors, γ, R_0 are the Sternheimer coefficients, that should consider antiscreening and screening processes of the probe nucleus by the internal electron shells of the probe atom from external charges.

Blaha et al., suggested the full potential linearised-augmented-plane-wave (LAPW) method for the theoretical calculation of the parameters of the total EFG tensor using the local-density-approximation (LDA) (Blaha et al. 1985). This calculation is carried out without additional approximations such as the Sternheimer antishielding coefficients. Using this approach, EFG calculations "from first principles" based on LDA for high-temperature superconductors $YBa_2Cu_3O_7$ (Schwarz et al. 1990) were performed. When using the X-ray diffraction data (Beno et al. 1987) for $YBa_2Cu_3O_7$ and the nuclear quadrupole moment Q = –0.211 b for ^{63}Cu and Q = –0.026 b for ^{17}O while converting NQR frequencies to EFG, the calculated EFGs were in good agreement with the experimental NQR measurements with ^{63}Cu (Pennington et al. 1989), ^{17}O (Takigawa et al. 1989) and ^{137}Ba (Shore et al. 1992) for Ba, Cu, and O sites, with the exception of the planar copper Cu(2) nodes, where the main component of the experimental EFG tensor is more than twice the calculated value. Similar results were also presented in (Yu et al. 1991). In connection with this discrepancy, the authors of (Ambrosch-Draxl et al. 1991) reported on EFG calculations for $YBa_2Cu_3O_7$, in which the ambiguities presented in LAPW were eliminated. Despite the changes in the calculations, the calculated EFG at the Cu(2) site is similar to the values obtained in earlier LAPW studies. This means that the discrepancy between the EFG calculated within the LDA framework and the experimental one cannot be explained by a computational artefact and confirms the assumption made in (Schwarz et al. 1990), that the discrepancy is a real LDA error. It is emphasised that the EFG tensor components are only the second derivatives of the Coulomb potential and thus represent well-defined properties of the ground state, uniquely determined by the charge density.

It can be noted here that the studies of $La_{2-x}Sr_xCuO_4$ performed in (Sun et al. 2015; 2016) demonstrate how the doping electronic structures of high-temperature cuprate superconductors can be accurately modelled based on the first principles developed in (Lee et al. 2021). These calculations correctly predict the key experimentally observed features of the electronic structure and magnetism of $La_{2-x}Sr_xCuO_4$ without involving any free parameters. Thus, studies (Lee et al. 2021; Sun et al. 2016) open a new way to investigate the first principles of electronic structures and broader properties of correlated materials in general.

It is possible to just compare the theoretical and experimental parameters of the lattice EFG tensor to determine the effective charges of atoms (Marchenko et al. 2018a; 2018b; Terukov et al. 2018). If the electron shells of the probe atom are completely (or half) filled, then the electron cloud can be considered as consisting of several concentric spheres. The strength of the electrostatic field from such spheres on the nucleus is zero, so only the charges of the neighbouring atoms should be taken into consideration when calculating the EFG at the nucleus of an atom-probe (lattice probe).

The method of making lattice EFG tensor calculations using the point charge model is quite simple and clear. For such a calculation, only the unit cell parameters are required, which are known for most HTSCs from X-ray diffraction studies. The term "effective charges" refers to the charges that are required to describe the electric field of ions using the Coulomb potential. Effective charges accurately present the valence states of ions at the lattice sites and the significant deviations from their standard valence states (Seregin, Masterov, Nasredinov 1992; Seregin, Marchenko, Seregin et al. 1992; 2015). Such calculations for the $YBa_2Cu_3O_7$ and $La_{2-x}Sr_xCuO_4$ lattices have been carried out in many works (see, for example, (Adrian 1989; Garcia, Bennemann 1989; Lyubutin et al. 1989; Seregin et al. 1992; 2015; Shimizu 1993)), but their results are in poor agreement with experimental data (Ishida et al. 1991; Masterov et al. 1995; Ohsugi 1995; Ohsugi et al. 1994; Pennington et al. 1989; Shore et al. 1992; Takigawa et al. 1989).

This is explained by the fact that copper metal oxides $YBa_2Cu_3O_7$ and $La_{2-x}Sr_xCuO_4$ predominantly contain atoms that do not form lattice probes.

This study describes effective charge determination for atoms in the copper metal oxides $YBa_2Cu_3O_7$ and $La_{2-x}Sr_xCuO_4$. The calculated EFG tensor parameters are compared with the experimental NQI tensor parameters measured by NMR/NQR or MS using the lattice probes located at the lattice sites. The EFG tensor parameters are the main components of the lattice EFG tensors at the *i*-sites of the lattice V_{zzi} and the asymmetry parameters of these tensors η_{lati}. The parameters of the NQI tensors are the quadrupole interaction constants $C_{expi} = Q_i(1 - \gamma_i)V_{zzi} = \alpha_i V_{zzi}$ and the asymmetry parameters η_{expi} (here $\alpha_i = Q_i(1 - \gamma_i)$ is the electron-nuclear parameter of the lattice *i*-probe located at the *i*-site of the lattice, γ_i is the Sternheimer coefficient of the *i*-probe and Q_i is the quadrupole moment of the atomic nucleus of the *i*-probe).

Requirements for lattice probes

There are several requirements for the lattice probes (Seregin et al. 2015):

- it is necessary to use such probes that their position in the lattice is known a priori;
- the possibility of uncontrolled appearance of point defects in the lattice (such as vacancies or atoms displaced into interstitial spaces) is excluded during probe introduction. Such defects distort the results of EFG tensor calculations;
- to eliminate any uncertainties in the theoretical values of nucleus quadrupole moments and Sternheimer coefficients, as well as to determine the effective charges of atoms in units of electron charge, it is necessary to experimentally determine the coefficient $\alpha = eQ(1 - \gamma)$ for at least one probe that is used;
- to reduce the influence that coefficient α uncertainties have on the values of the obtained effective charges, it is appropriate to use the minimum number of probes and, in the ideal case, use one probe each in the cationic and anionic sublattices (of course, each probe should replace as many crystallographically nonequivalent sites of the crystal lattice as possible);
- for crystals containing one lattice probe in two crystallographically non-equivalent positions, one should not compare the values V_{zzi} and $C_{expi} = eQ_i(1 - \gamma_i)V_{zzi}$, but the values of the ratios V_{zz1}/V_{zz2} and C_{exp1}/C_{exp2}, where V_{zz1}, V_{zz2} are the principal components of the lattice EFG tensor at structurally nonequivalent sites 1 and 2 occupied by the lattice probe atom, and C_{exp1} and C_{exp2} are the quadrupole interaction constants for the lattice probe at these sites (i.e., it is proposed to exclude quadrupole moments of probe nuclei and Sternheimer coefficients of probe atoms);
- All of these conditions for $YBa_2Cu_3O_7$ and $La_{2-x}Sr_xCuO_4$ are satisfied for the $^{67}Zn^{2+}$ probe using emission MS (Seregin et al. 2015);
- when using emission MS with $^{67}Cu(^{67}Zn)$ isotopes, copper atoms form a lattice probe of divalent zinc $^{67}Zn^{2+}$ after beta decay of ^{67}Cu at the sites of divalent copper Cu^{2+} in the $YBa_2Cu_3O_7$ and $La_{2-x}Sr_xCuO_4$ lattices;
- when using emission MS with $^{67}Ga(^{67}Zn)$ isotopes, trivalent gallium atoms $^{67}Ga^{3+}$ replace trivalent yttrium atoms Y^{3+} in the $YBa_2Cu_3O_7$ lattice or trivalent lanthanum atoms La^{3+} in the $La_{2-x}Sr_xCuO_4$ lattice, and the lattice probe of bivalent zinc $^{67}Zn^{2+}$ stabilises at trivalent yttrium (or trivalent lanthanum) sites after the electron capture in ^{67}Ga.

The results of Mössbauer spectroscopy of the $YBa_2Cu_3O_7$ compound (Seregin et al. 2015) show that in some structural positions the oxygen atom can be considered a $^{17}O^{2-}$ lattice probe, making it possible to determine the effective charges of all atoms in the $YBa_2Cu_3O_7$ and $La_{2-x}Sr_xCuO_4$ crystal lattices using the NQR data with the ^{17}O isotope (Masterov et al. 1995; Terukov et al. 2018).

To confirm the validity of the effective charges determined in $La_{2-x}Sr_xCuO_4$, other lattice probes can also be introduced:

- when using emission MS with $^{57}Co(^{57m}Fe)$ isotopes, the atoms of bivalent cobalt Co^{2+} replace the atoms of bivalent copper Cu^{2+} in the $La_{2-x}Sr_xCuO_4$ lattice, and the lattice probe of trivalent iron $^{57m}Fe^{3+}$ is stabilised at the sites of bivalent copper after electron capture in ^{57}Co;
- when using emission MS with $^{155}Eu(^{155}Gd)$ isotopes, the trivalent europium atoms $^{155}Eu^{3+}$ replace the atoms of trivalent lanthanum La^{3+} in the $La_{2-x}Sr_xCuO_4$ lattice, and the lattice probe of trivalent gadolinium $^{155}Gd^{3+}$ is stabilised at the sites of trivalent lanthanum after the decay of ^{155}Eu.

 https://www.doi.org/10.33910/2687-153X-2022-3-2-86-99

Experimental techniques

EFG tensors calculations

Copper oxide Cu_2O and superconducting $YBa_2Cu_3O_7$ and $La_{2-x}Sr_xCuO_4$ ceramics were chosen as objects of study.

The Cu_2O compound crystallises in a cubic lattice (Wells 1984). The $YBa_2Cu_3O_7$ compound has an orthorhombic structure (see Fig. 1a) (Yvon, Francois 1989). The $La_{2-x}Sr_xCuO_4$ solid solutions crystallise in a lattice of the K_2NiF_4 type (a weakly distorted orthogonal structure; for $x > 0.1$, the lattice becomes tetragonal (see Fig. 1b) (Yvon, Francois 1989).

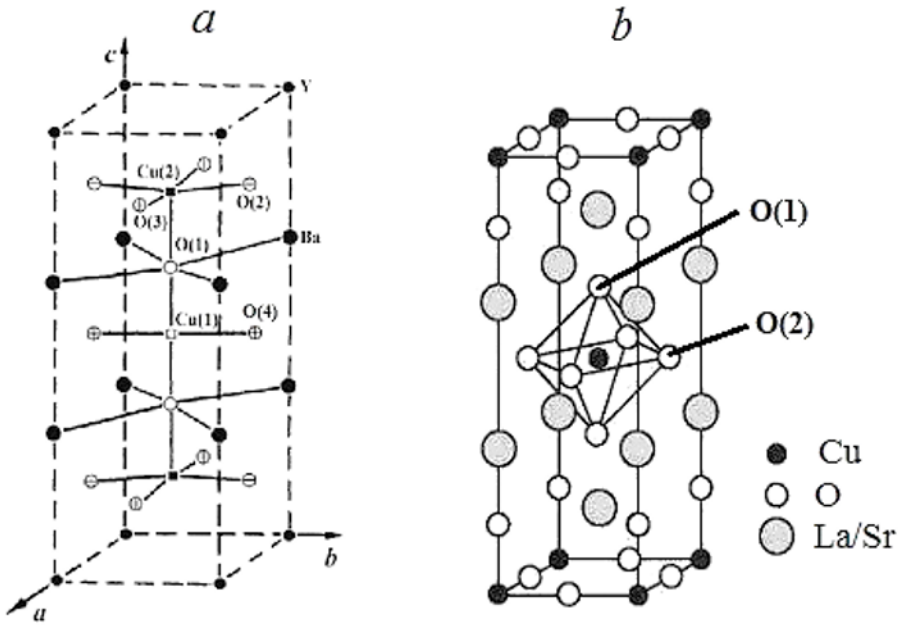

Fig. 1. Unit cells of $YBa_2Cu_3O_7$ (a) and $La_{2-x}Sr_xCuO_4$ (b)

The components of the lattice EFG tensor were calculated using the point-charge model with the relations (Seregin et al. 2015).

$$V_{\alpha\alpha} = \sum_k e_k \sum_i \frac{1}{r_{ki}^3}\left[\frac{3\alpha_{ki}^2}{r_{ki}^2} - 1\right] = \sum_k e_k G_{\alpha\alpha k},$$
$$V_{\alpha\beta} = \sum_k e_k \sum_i \frac{3\alpha_{ki}\beta_{ki}}{r_{ki}^5} = \sum_k e_k G_{\alpha\beta k} \qquad (4)$$

where k is the summation index over sublattices, i is the summation index over sublattice sites, α, β are the Cartesian coordinates, e_k are the effective charges of atoms of the k-sublattice (in units of the electron charge e), r_{ki} is the distance from the i-ion of the k-sublattice to node where the EFG is calculated.

The lattice of the Cu_2O compound was represented as Cu_4O_2, and the atomic coordinates c and unit cell parameters were set according to (Wells 1984).

According to (Yvon, Francois 1989), a unit cell of the $YBa_2Cu_3O_7$ compound contains nodes of yttrium, barium, chain copper Cu(1), planar copper Cu(2), apical oxygen O(1), planar oxygen O(2), O(3) and chain O(4) oxygen (see Fig. 1a). The $YBa_2Cu_3O_7$ lattice was represented as $YBa_2Cu(1)Cu(2)_2O(1)_2O(2)_2O(3)_2O(4)$, and the summation index over sublattices in the formula (3) took the following values:

k =	1	2	3	4	5	6	7	8
atom	Y	Ba	Cu(1)	Cu(2)	O(1)	O(2)	O(3)	O(4)

According to (Yvon, Francois 1989), a unit cell of $La_{2-x}Sr_xCuO_4$ solid solution contains nodes of lanthanum (strontium), copper, apical O(1) and planar oxygen O(2) (see Fig. 1b). The $La_{2-x}Sr_xCuO_4$ lattice was represented as in the form $(La,Sr)_2CuO(l)_2O(2)_2$, with the crystallographic parameters taken from (Yvon, Francois 1989; Tarascon et al. 1987); the summation index over sublattices in the formula (3) took the following values:

k =	1	2	3	4	5
atom	La	Sr	Cu	O(1)	O(2)

The tensors $G_{\alpha\alpha}$ and $G_{\beta\beta}$ were calculated inside spheres with a radius of 30 Å, and the obtained parameters of the tensors are consistent with the literature data (Seregin et al. 2015).

Sample synthesis and Mössbauer spectra measurement

Cu_2O copper oxide was obtained by calcining CuO in vacuum. $YBa_2Cu_3O_7$ and $La_{2-x}Sr_xCuO_4$ compounds ($x = 0 \div 1$) were prepared using ceramic technology (Seregin et al. 2015). The $YBa_2Cu_3O_7$ samples had an orthorhombic structure, while the $La_{2-x}Sr_xCuO_4$ samples had a K_2NiF_4 type structure. The obtained materials were single-phase with superconducting transition temperatures of 91 K for $YBa_2Cu_3O_7$ and 25, 37, 32 K for $La_{2-x}Sr_xCuO_4$ (where x = 0.1, 0.15, 0.2). Ceramics were alloyed with isotopes ^{67}Cu, ^{67}Ga, ^{57}Co and ^{155}Eu during diffusion annealing (Seregin et al. 2015).

Mössbauer spectra were recorded at 80 K (^{57}Co, ^{155}Eu) and 4.2 K (^{67}Cu, ^{67}Ga) with $K_4{}^{57}Fe(CN)_6.3H_2O$, $^{155}GdPd_3$, and ^{67}ZnS absorbers.

Table 1. Experimental NQI parameters at the lattice sites of $YBa_2Cu_3O_7$, $La_{1.85}Sr_{0.15}CuO_4$, and Cu_2O

Compound	Node	Probe	Method	C_{exp},MHz	η_{exp}	z-axis of the EFG tensor	Reference
$YBa_2Cu_3O_7$	Y	^{67}Zn	MS $^{67}Ga(^{67}Zn)$	−2.2(3)	0.8(1)	c	[*]
	Ba	^{137}Ba	NQR ^{137}Ba	|56.4(1)|	0.94(2)	c	[6]
	Cu(1)	^{67}Zn	MS $^{67}Cu(^{67}Zn)$	+20.1(3)	0.95(3)		[*]
	Cu(2)	^{67}Zn	MS $^{67}Cu(^{67}Zn)$	+11.8(3)	≤ 0.2		[*]
	O(1)	^{17}O	NMR ^{17}O	|7.3(1)|	0.32(2)	c	[2]
	O(2)	^{17}O	NMR ^{17}O	|6.4(1)|	0.24(2)	b	[2]
	O(3)	^{17}O	NMR ^{17}O	|6.6(1)|	0.21(2)	a	[2]
	O(4)	^{17}O	NMR ^{17}O	|10.9(1)|	0.41(2)	b	[2]
$La_{1.85}Sr_{0.15}CuO_4$	La,Sr	^{67}Zn	MS $^{67}Cu(^{67}Zn)$	−2.7(2)	≤ 0.2		[*]
	Cu	^{67}Zn	MS $^{67}Cu(^{67}Zn)$	11.4(5)	≤ 0.2		[*]
	O(1)	^{17}O	NMR ^{17}O	|1.33(5)|	0.0		[3]
	O(2)	^{17}O	NMR ^{17}O	|4.6(1)|	0.36(2)		[3]
Cu_2O	Cu	^{67}Zn	MS $^{67}Cu(^{67}Zn)$	−22.0(3)	≤ 0.2		[*]

[*]—the results of this work.

https://www.doi.org/10.33910/2687-153X-2022-3-2-86-99

Experimental results and discussion

MS data

The Mössbauer spectra of ^{67}Zn are shown in Figs. 2–4, the results of their processing are summarised in Table 1. The same table shows NQR data for barium (Shore et al. 1992) and oxygen (Ishida et al. 1991; Takigawa et al. 1989) sites.

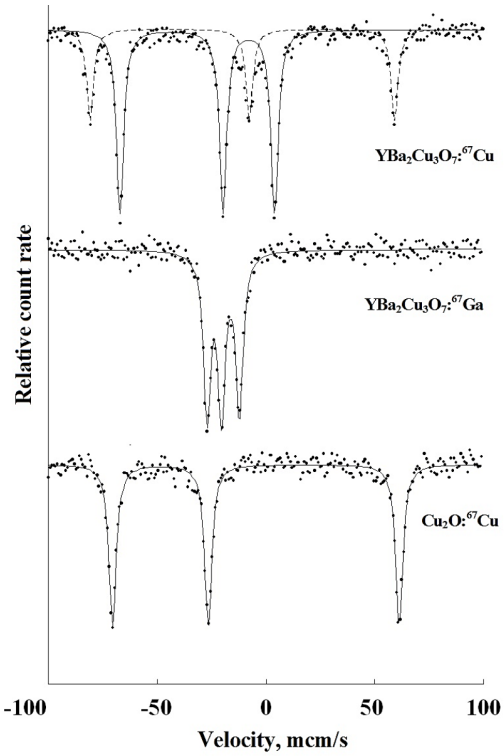

Fig. 2. ^{67}Cu(^{67}Zn) and ^{67}Ga(^{67}Zn) Mössbauer spectra of $YBa_2Cu_3O_7$ and Cu_2O compounds at 4.2 K

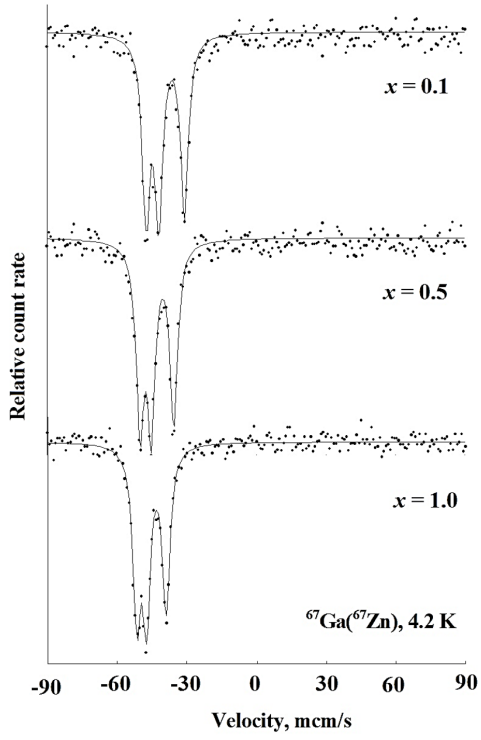

Fig. 3. ^{67}Cu(^{67}Zn) Mössbauer spectra of $La_{2-x}Sr_xCuO_4$ solid solutions for x = 0.1, 0.5, and 1.0 at 4.2 K

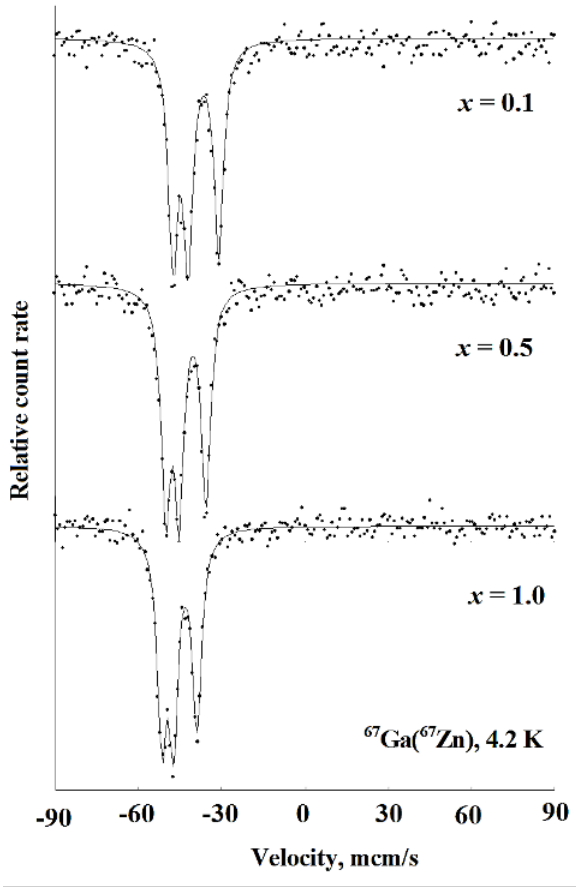

Fig. 4. ^{67}Ga(^{67}Zn) Mössbauer spectra of $La_{2-x}Sr_xCuO_4$ solid solutions for x = 0.1, 0.5, and 1.0 at 4.2 K

The Mössbauer emission spectra of ^{67}Cu(^{67}Zn) and ^{67}Ga(^{67}Zn) of all studied materials are either well-resolved quadrupole triplets (spectra of Cu_2O:^{67}Cu, $YBa_2Cu_3O_7$:^{67}Ga (see Fig. 2), $La_{2-x}Sr_xCuO_4$:^{67}Cu (see Fig. 3), and $_{2-x}Sr_xCuO_4$:^{67}Ga (see Fig. 4)), or a superposition of two quadrupole triplets ($YBa_2Cu_3O_7$:^{67}Cu spectrum (see Fig. 2)). According to the values of isomer shifts, these spectra correspond to the lattice centres of divalent zinc $^{67}Zn^{2+}$ either at copper sites (^{67}Cu(^{67}Zn) spectra) or at yttrium and lanthanum sites (^{67}Ga(^{67}Zn) spectra). The number of quadrupole triplets in the experimental spectra is determined by the number of crystallographic positions occupied by the substituting atoms.

The ^{57}Co(^{57m}Fe) and ^{155}Eu(^{155}Gd) Mössbauer emission spectra of $La_{2-x}Sr_xCuO_4$ solid solutions are quadrupole triplets (see Figs. 5 and 6). According to the values of isomeric shifts, these spectra correspond to the lattice centres of trivalent iron $^{57m}Fe^{3+}$ and trivalent gadolinium $^{155}Gd^{3+}$ at lanthanum sites.

The noncubic symmetry of the local environment of copper, yttrium, and lanthanum atoms leads to the splitting of the spectra into quadrupole triplets (^{67}Cu(^{67}Zn) and ^{67}Ga(^{67}Zn) spectra) or quadrupole doublets (^{57}Co(^{57m}Fe) and ^{155}Eu(^{155}Gd) spectra).

https://www.doi.org/10.33910/2687-153X-2022-3-2-86-99

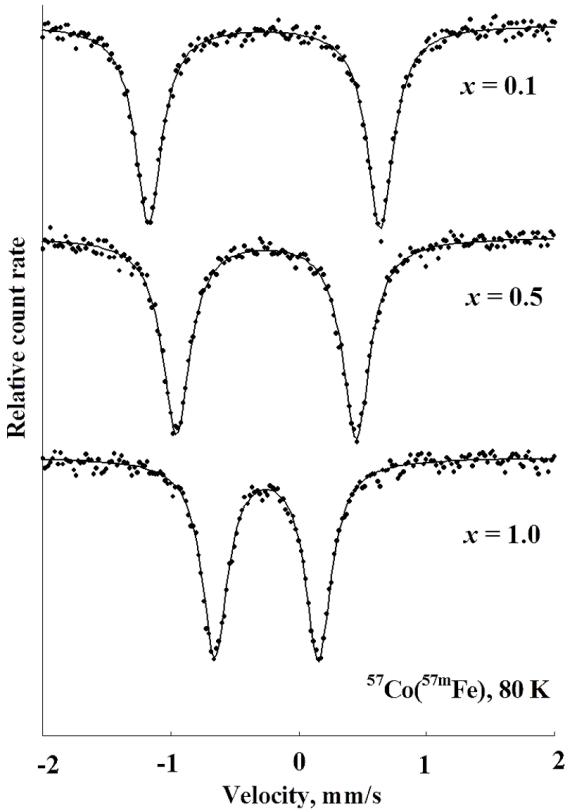

Fig. 5. ^{57}Co(^{57m}Fe) Mössbauer spectra of $La_{2-x}Sr_xCuO_4$:^{57}Co for x = 0.1, 0.5, and 1.0 at 80 K

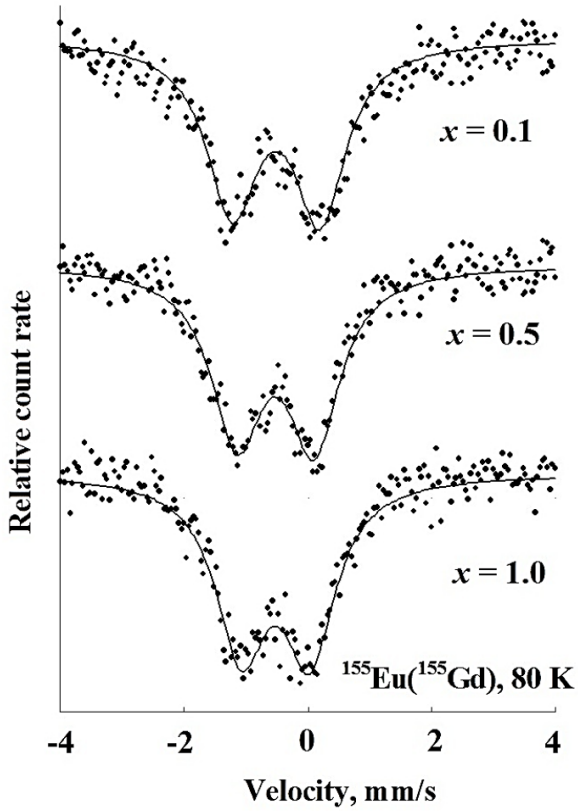

Fig. 6. ^{155}Gd Mössbauer spectra of $La_{2-x}Sr_xCuO_4$:^{155}Eu solid solutions for x = 0.1, 0.5, and 1.0 at 80 K

Determining the $\alpha_{Zn} = eQ_{Zn}(1 - \gamma_{Zn})$ coefficient for the $^{67}Zn^{2+}$ probe

For the $Cu^{+}_{2}O^{2-}$ model, the calculation for copper sites yields $V_{zz} = -1.093$ e/Å^3, which leads to α_{Zn} equal to 20.1(3) MHz.Å^3/e for ^{67}Zn=– centres at copper sites in the Cu_2O lattice.

Determining effective atom charges in the $YBa_2Cu_3O_7$ lattice

To determine the effective charges of $YBa_2Cu_3O_7$ lattice atoms, emission MS data on the isotopes ^{67}Cu(^{67}Zn) and ^{67}Ga(^{67}Zn) and NQR data on the isotope ^{17}O were used (Takigawa et al. 1989).

A system of equations was compiled, including

- the equation of electroneutrality:

$$e_1 + 2e_2 + e_3 + 2e_4 + 2e_5 + 2e_6 + 2e_7 + e_8 = 0, \quad (5)$$

- the equation relating the quantities V_{zz1}. and C_1 for the $^{67}Zn^{2+}$ probe at yttrium nodes:

$$\alpha_{Zn} \sum_{k=1}^{k=8} e_k G_{zzk1} = C_1, \quad (6)$$

- the equation relating the quantities V_{zz3}/V_{zz4} and $P_{34} = C_3/C_4$ for the $^{67}Zn^{2+}$ probe at the Cu(1) and Cu(2) sites:

$$\sum_{k=1}^{k=8} e_k \left[G_{zzk3} - P_{34} G_{zzk4} \right] = 0, \quad (7)$$

- equation relating the values V_{zz5}/V_{zz6} and $P_{56} = C_5/C_6$ for the $^{17}O^{2-}$ probe at the O(5) and O(7) nodes:

$$\sum_{k=1}^{k=8} e_k \left[G_{zzk5} - P_{56} G_{zzk6} \right] = 0, \quad (8)$$

- four equations relating the calculated and experimental values of the asymmetry parameters of the EFG tensors for the $^{67}Zn^{2+}$ probe at the copper sites and for the $^{17}O^{2-}$ probe at the O(1) and O(2) sites:

$$\sum_{k=1}^{k=8} e_k \left[G_{xxkl} - G_{yykl} - \eta_l G_{zzkl} \right] = 0, \quad (9)$$

where l = 3, 4, 5, 6.

Additional factors that were taken into account are as follows:

- the principal axes of the EFG tensors for the $^{17}O^{2-}$ centres at the O(1) and O(2) sites coincide with the crystallographic axes *c* and *b*, respectively (Takigawa et al. 1989);
- the main axis of the EFG tensor for $^{137}Ba^{2+}$ centres is directed along the crystallographic *c* axis (Shore et al. 1992);
- the main axis of the EFG tensor for $^{155}Gd^{3+}$ centres at Y sites is directed along the crystallographic *c* axis (Wortmann et al. 1989);
- solutions with negative charges of cations or positive charges of anions were rejected as having no physical meaning.

The accuracy of effective charge e_k values obtained from the system of equations (5–9) is limited by the assumption that there is no valence electric field on probe nuclei. As an example, Table 2 shows the atom charges obtained using the experimental values from Table 1 and various structural data (Capponi et al. 1987; Francois et al. 1988; Konstatntinovic et al. 1989; Le Page et al. 1987; Yvon, Francois 1989). The reduced values of the O(4) and O(3) charges reflect charge distribution in the $YBa_2Cu_3O_7$ lattice,

 https://www.doi.org/10.33910/2687-153X-2022-3-2-86-99

while the deviations of remaining atoms' charges from the standard oxidation states are random and are associated with the difference in the temperatures for determining the NQI parameters and the parameters of the $YBa_2Cu_3O_7$ crystal lattice structure, and also with the errors in the latter.

Table 2. Effective charges of atoms of the $YBa_2Cu_3O_7$ lattice obtained by solving the system of equations (5–9) with different structural data at different temperatures

Structural data	T, K	e1	e2	e3	e4	e5	e6	e7	e8	Model
[28]	5 K	2.92	2.04	1.96	2.00	–2.09	–1.93	–1.81	–1.28	1
[28]	320 K	2.80	1.90	1.88	1.92	–1.99	–1.83	–1.71	–1.22	2
[29]	5 K	2.91	2.01	1.88	1.99	–2.05	–1.92	–1.80	–1.25	3
[31]	298 K	3.03	2.06	2.13	2.14	–2.18	–2.00	–1.91	–1.36	4
[30]	9 K	2.99	2.00	2.01	2.00	–2.00	–2.00	–1.80	–1.40	5
[25]	295K	3.00	1.99	2.00	2.01	–2.00	–2.00	–1.85	–1.30	6

The models given in Table 2 satisfy the assumption made in (Baryshev et al. 2011; Mitsen, Ivanenko 2007) about the localisation of holes in $YBa_2Cu_3O_{7-x}$ around Cu ions in CuO_3 chains on oxygen ions (O(4) crystallographic position).

For all models from Table 2, the calculated parameters of the lattice EFG tensors with different structural data turn out to be similar. For model 6, these values are shown in Table 3.

Table 3. Components of lattice EFG tensors for $YBa_2Cu_3O_7$ crystal sites (model 6)

Node	Vaa, e/Å3	Vbb, e/Å3	Vcc, e/Å3	ηlat
Y	0.006	0.107	– 0.113	0.89
Ba	– 0.118	– 0.003	0.121	0.94
Cu(1)	0.982	– 0.036	– 0.946	0.97
Cu(2)	– 0.263	– 0.324	0.587	0.10
O(1)	– 0.158	– 0.331	0.489	0.35
O(2)	– 0.153	0.385	– 0.232	0.21
O(3)	0.439	– 0.206	– 0.233	0.06
O(4)	– 0.086	0.575	– 0.489	0.70

The obtained parameters of the lattice EFG tensors can be used to interpret NQR data on the ^{137}Ba isotope, for which the value C_{exp} = 56.4MHz, η_{exp} = 0.94 was found in $YBa_2Cu_3O_7$ (Shore et al. 1992). We calculated the lattice EFG tensor at Ba nodes for model 6 in Table 3. For the $^{137}Ba^{2+}$ probe, the value $\alpha_{Ba} = e\,Q\,(1-\gamma)$ = 470(9) MHz.e/Å^3 was obtained.

Similarly, the value $\alpha_O = e\,Q\,(1-\gamma)$ can be determined for lattice centres $^{17}O^{2-}$. Using the values V_{zz5} (see Table 3) and C_5 (see Table 1) for the $^{17}O^{2-}$ centers at the nodes O(1) of the $YBa_2Cu_3O_7$ lattice, we obtained α_O = 14.9(2) MHz.Å^3/e.

Finally, we obtained $z \,||\, c$ and $U_{zz} < 0$ for the $^{155}Gd^{3+}$ lattice probe in the $YBa_2Cu_3O_7$ compound within the framework of the point charge model (see Table 3). This is in agreement with MS results (Wortmann et al. 1989) obtained on the ^{155}Gd isotope for the compound $GdBa_2Cu_3O_7$.

Effective atom charges in the lattices of $La_{2-x}Sr_xCuO_4$ solid solutions

To determine the effective atom charges in the $La_{2-x}Sr_xCuO_4$ lattice, we used emission MS data on the ^{67}Cu(^{67}Zn) and ^{67}Ga(^{67}Zn) isotopes, as well as NQR data on the ^{17}O isotope (Ishida et al. 1991). It should be noted that according to the data on the ^{17}O isotope, the asymmetry parameter of the EFG tensor for planar oxygen O(2) lattice $La_{1.85}Sr_{0.15}CuO_4$ is different from zero (see Table 1), whereas according to the calculations of the lattice EFG tensor for this oxygen, η_4 = 0. In other words, the crystal probe can only be the apical oxygen centre O(1).

Thus, the following system of equations was compiled:

- the equation of electroneutrality:

$$2e_1 + e_2 + 2e_3 + 2e_4 = 0, \quad (10)$$

- the equation relating the quantities V_{zz1}. and C_1 for the $^{67}Zn^{2+}$ probe at lanthanum nodes:

$$\alpha_{Zn} \sum_{k=1}^{k=4} e_k G_{zzk1} = C_1, \quad (11)$$

- the equation relating the quantities V_{zz2}. and C_2 for the $^{67}Zn^{2+}$ probe at copper nodes;

$$\alpha_{Zn} \sum_{k=1}^{k=4} e_k G_{zzk2} = 0, \quad (12)$$

where α_{Zn} = 20.1(3) MHz.Å^3/e.

- the equation relating the quantities V_{zz3}. and C_3 for the $^{17}O^{2-}$ probe at O(1) nodes;

$$\alpha_{\text{î}} \sum_{k=1}^{k=4} e_k G_{zzk3} = 0, \quad (13)$$

where α_O = 14.9(2) MHz.Å^3/e.

The effective charges of metal atoms and apical oxygen atoms of the $La_{2-x}Sr_xCuO_4$ lattice, as in the case of the $YBa_2Cu_3O_7$ lattice, correspond to the standard oxidation states of these atoms. However, for planar oxygen atoms, a reduced charge of planar oxygen atoms is observed, which is consistent with the authors' assumption (Baryshev et al. 2011; Mitsen, Ivanenko 2007) about the localisation of a hole in the energy zone formed by the electronic states of O(2) atoms. Taking into account the error in determining the parameters of the lattice GAP tensors, the distribution of atomic charges in the $La_{2-x}Sr_xCuO_4$ lattice can be represented as

$$(La_{1.85}Sr_{0.15})^{2.925+}Cu^{2+}O(1)^{2-}{}_2(2)^{1.925-}{}_2. \quad (13)$$

To confirm the model (13), we performed a co-representation of the calculated $P(x) = [V_{zz}]_x/[V_{zz}]_{x=0.1}$ and experimental $P_{exp} = [eQU_{zz}]_x/[eQU_{zz}]_{x=0.1}$ dependencies in lanthanum nodes (see Fig. 7) and copper (see Fig. 8) lattices of $La_{2-x}Sr_xCuO_4$ solid solutions. MS was used on isotopes $^{57}Co(^{57m}Fe)$, $^{67}Cu(^{67}Zn)$ (see Fig. 7) and $^{67}Ga(^{67}Zn)$, $^{155}Eu(^{155}Gd)$ (see Fig. 8). The indicated permutations were carried out for four models of hole localisation: the hole is located in the sublattice of copper; in the sublattice of apical oxygen; in the sublattice of planar oxygen and the hole is distributed between sublattices of apical and planar oxygen. The dependences of P(x) in Figs. 7 and 8 can be explained if the hole is localised mainly in the positions of planar oxygen.

Conclusion

Using only crystallographic data, Mossbauer spectroscopy data on the ^{67}Zn isotope and nuclear quadrupole resonance on the ^{17}O isotope, as well as calculations of lattice EFG tensors, the effective charges of all atoms of superconducting copper metal oxide $YBa_2Cu_3O_7$ and $La_{2-x}Sr_xCuO_4$ lattices were determined. These charges correspond to the standard degrees of atom oxidation, with the exception of the chain and planar oxygen atoms in the $YBa_2Cu_3O_7$ lattice and planar oxygen atoms in the $La_{2-x}Sr_xCuO_4$ lattice. The reduced charge of these atoms is explained by the localisation of holes in the corresponding sublattices.

 https://www.doi.org/10.33910/2687-153X-2022-3-2-86-99

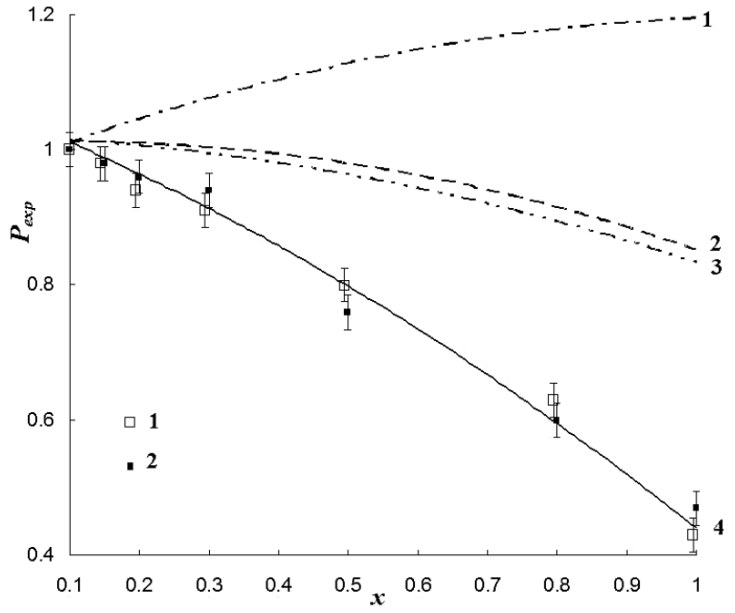

Fig. 7. Dependences of P_{exp} on x for $La_{2-x}Sr_xCuO_4$ for copper sites: (1) the hole is located in the copper sublattice; (2) the hole is in the O(1) sublattice; (3) the hole is in the O(2) sublattice; (4) the hole is distributed between the O(1) and O(2) sublattices; open and filled squares are experimental MS data with the $^{57}Co(^{57m}Fe)$ (1) and $^{67}Cu(^{67}Zn)$ (2) isotopes

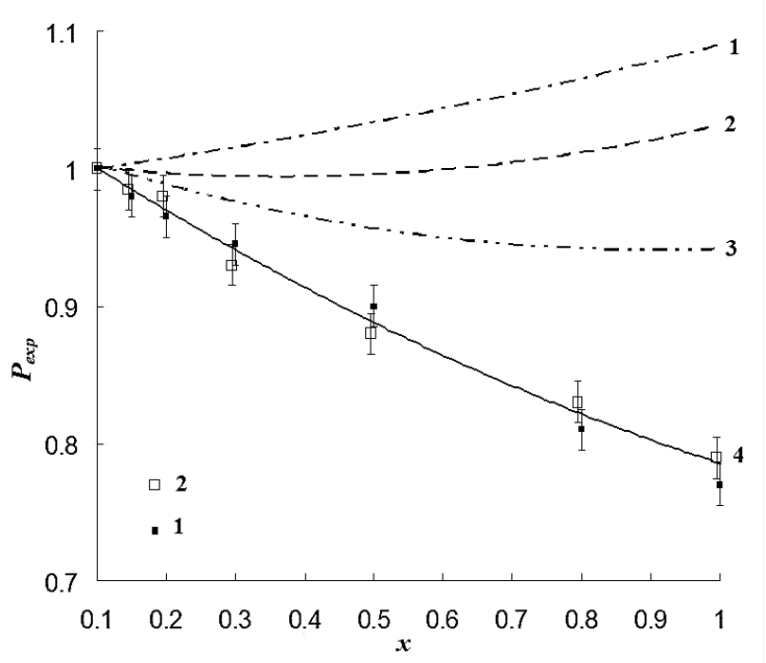

Fig. 8. Dependences of P_{exp} on x for $La_{2-x}Sr_xCuO_4$ for lanthanum sites: 1—the hole is localised in Cu positions; 2—the hole is localised in positions O(1); 3—the hole is localised in positions O(2); 4—the hole is localised in positions O(1) and O(2); open and filled squares are experimental data with the $^{67}Ga(^{67}Zn)$ (1) and $^{155}Eu(^{155}Gd)$ (2) isotopes

Conflict of Interest

The authors declare that there is no conflict of interest, either existing or potential.

References

Adrian, F. J. (1989) Structural implications of nuclear electric quadrupole splittings in high-T_c superconductors. *Physical Review B*, 38 (4), 2426–2431. https://doi.org/10.1103/physrevb.38.2426 (In English)

Ambrosch-Draxl, C., Blaha, P., Schwarz, K. (1991) Electronic structure and electric-field gradients for $YBa_2Cu_4O_8$ from density-functional calculations. *Physical Review B*, 44 (10), 5141–5147. https://doi.org/10.1103/physrevb.44.5141 (In English)

Baryshev, S. V., Kapustin, A. I., Bobyl, A. V. et al. (2011) Temperature dependences of $YBa_2Cu_3O_x$ and $La_{2-x}Sr_xCuO_4$ resistivity in terms of the negative-U centers model. *Superconductor Science and Technology*, 24, article 075026. https://doi.org/10.1088/0953-2048/24/7/075026 (In English)

Bednorz, J. G., Muller, K. A. (1986) Possible high T_c superconductivity in the Ba–La–Cu–O system. *Zeitschrift für Physik B Condensed Matter*, 64, 189–193. https://doi.org/10.1007/BF01303701 (In English)

Beno, M. A., Soderholm, L., Capone, D. W. et al. (1987) Structure of the single-phase high-temperature superconductor $YBa_2Cu_3O_{7-\delta}$. *Applied Physics Letters*, 51 (1), 57–60. https://doi.org/10.1063/1.98886 (In English)

Blaha, P., Schwarz, K., Herzig, P. (1985) First-principles calculation of the electric field gradient of Li_3N. *Physical Review Letters*, 54 (11), 1192–1198. https://doi.org/10.1103/PhysRevLett.54.1192 (In English)

Capponi, J. J., Chaillout, C., Hewat, A. W. et al. (1987) Structure of the 100 K superconductor $Ba_2YCu_3O_7$ between (5–300) K by neutron powder diffraction. *Europhysics Letters*, 3 (12), 1301–1307. https://doi.org/10.1209/0295-5075/3/12/009 (In English)

Francois, M., Junod, A., Yvon, K. et al. (1988) A study of the Cu-O chains in the high T_c superconductor $YBa_2Cu_3O_7$ by high resolution neutron powder diffraction. *Solid State Communications*, 66 (10), 1117–1125. https://doi.org/10.1016/0038-1098(88)90335-3 (In English)

Garcia, M. E., Bennemann, K. H. (1989) Theoretical study of the structural dependence of nuclear quadrupole frequencies in high-T_c superconductors. *Physical Review B*, 40 (13), 8809–8813. https://doi.org/10.1103/PhysRevB.40.8809 (In English)

Ishida, K., Kitaoka, Y., Zheng, G., Asayama, K. (1991) ^{17}O and ^{63}Cu NMR Investigations of high-T_c superconductor $La_{1.85}Sr_{0.15}CuO_4$ with T_c = 38 K. *Journal of the Physical Society of Japan*, 60 (10), 3516–3524. https://doi.org/10.1143/JPSJ.60.3516 (In English)

Konstatntinovic, J., Parette, G., Djordjevic, Z., Menelle, A. (1989) Structural transformations of the $YBa_2Cu_3O_{6.84}$ crystal lattice in the temperatute interval 9 K to 300 K. *Solid State Communications*, 70 (2), 163–166. https://doi.org/10.1016/0038-1098(89)90967-8 (In English)

Lee, C. C., Chiu, J.-Y., Yamada-Takamura, Y. et al. (2021) Hidden competing phase revealed by first-principles calculations of phonon instability in the nearly optimally doped cuprate $La_{1.875}Sr_{0.125}CuO_4$. *Physical Review B*, 104 (6), article 064114. https://doi.org/10.1103/PhysRevB.104.064114 (In English)

Le Page, Y., Siegrist, T., Sunshine, S. A. et al. (1987) Structural properties of $Ba_2YCu_3O_7$ high-T_c superconductors. *Physical Review B*, 36 (7), 3617–3621. https://doi.org/10.1103/PhysRevB.36.3617 (In English)

Lyubutin, I. S., Terziev, V. G., Dmitrieva, T. V., Gor'kov, V. P. (1989) Lattice sum calculations and electric field gradients for orthorhombic and tetragonal phases of $YBa_2Cu_3O_x$. *Physics Letters A*, 137 (3), 144–148. https://doi.org/10.1016/0375-9601(89)90101-1 (In English)

Marchenko, A. V., Nasredinov, F. S., Kiselev, V. S., Seregin, P. P. (2018a) Analysis of the parameters of the Mössbauer spectra and the spectra of nuclear quadrupole resonance of the superconducting ceramic $YBa_2Cu_3O_7$. *Glass Physics and Chemistry*, 44 *(2)*, 92–99. https://doi.org/10.1134/S1087659618020116 (In English)

Marchenko, A. V., Nasredinov, F. S., Kiselev, V. S. et al. (2018b) Effective charges of atoms of HTSC $La_{2-x}Sr_xCuO_4$ ceramics determined from the analysis of the parameters of the nuclear quadrupole interaction. *Glass Physics and Chemistry*, 44 *(5)*, 412–417. https://doi.org/10.1134/S1087659618050115 (In English)

Masterov, V. F., Nasredinov, F. S., Seregin, P. P. (1995) Nuclear quadrupole interaction in high-temperature superconductors based on copper metal-oxides. *Physics of the Solid State*, 37, 1265–1292. (In English)

Mitsen, K., Ivanenko, O. (2007) The common origin of the pseudogap- and 60 K-phases in YBCO. *Physica C: Superconductivity*, 460–462 (2), 1094–1095. https://doi.org/10.1016/j.physc.2007.03.224 (In English)

Ohsugi, S. (1995) Doping dependence of the electric field gradiend at of La site in $La_{2-x}M_xCuO_4$ (M = Sr,Ba) La-NQR study. *Journal of the Physical Society of Japan*, 64 (10), 3656–3659. https://doi.org/10.1143/jpsj.64.3656 (In English)

Ohsugi, S., Kitaoka, Y., Ishida, K. et al. (1994) NMR study of magnetism and superconductivity in superconducting $La_{2-x}Sr_xCuO_4$. *Physica C: Superconductivity*, 235, 1633–1634. (In English)

Pennington, C. H., Durand, D. J., Slichter, C. P. (1989) Static and dynamic Cu NMR tensors of $YBa_2Cu_3O_{7-x}$. *Physical Review B*, 39 (4), 2902(R)–2905(R). https://doi.org/10.1103/PhysRevB.39.2902 (In English)

Schwarz, K., Ambrosch-Draxl, C., Blaha, P. (1990) Charge distribution and electric-field gradients in $YBa_2Cu_3O_{7-x}$. *Physical Review B*, 42 (4), 2051–2061. https://doi.org/10.1103/physrevb.42.2051 (In English)

Seregin, N. P., Masterov, V. F., Nasredinov, F. S. et al. (1992) Parameters of the electric field gradient tensor determined by ^{57}Co(^{57}Fe) and ^{67}Cu(^{67}Zn) emission Mossbauer spectroscopy for $La_{2-x}Sr_xCuO_4$ copper sites. *Superconductor Science and Technology*, 5 (11), 675–678. https://doi.org/10.1088/0953-2048/5/11/014 (In English)

Seregin, N. P., Marchenko, A. V., Seregin, P. P. (2015) *Emission Mössbauer spectroscopy. Electron defects and Bose-condensation in crystal lattices of high-temperature superconductors*. Saarbrücken: LAP Lambert Publ., 332 p. (In English)

Shimizu, T. (1993) On the electric Field Gradient at copper nuclei in oxides. *Journal of the Physical Society of Japan*, 62 (2), 772–778. https://doi.org/10.1143/JPSJ.62.772 (In English)

Shore, J., Yang, S., Haase, J. et al. (1992) Barium nuclear resonance spectroscopic study of $YBa_2Cu_3O_7$. *Physical Review B*, 46 (1), 595–598. https://doi.org/10.1103/physrevb.46.595 (In English)

Sun, J., Remsing, R. C., Zhang, Y. et al. (2016) Accurate first-principles structures and energies of diversely bonded systems from an efficient density functional. *Nature Chemistry*, 8, 831–836. https://doi.org/10.1038/nchem.2535 (In English)

Sun, J., Ruzsinszky, A., Perdew, J. P. (2015) Strongly constrained and appropriately normed semilocal density functional. *Physical Review Letters*, 115, article 036402. https://doi.org/10.1103/PhysRevLett.115.036402 (In English)

Takigawa, M., Hammel, P. C., Heffner, R. H. et al. (1989) ^{17}O NMR study of local spin susceptibility in aligned $YBa_2Cu_3O_7$ powder. *Physical Review Letters*, 63, 1865–1868. https://doi.org/10.1103/PhysRevLett.63.1865 (In English)

Tarascon, J. M., Greene, L. H., Mckinnon, W. R. et al. (1987) Superconductivity at 40 K in the oxygen-defect $La_{2-x}Sr_xCuO_{4-y}$. *Science*, 235 (4794), 1373–1376. https://doi.org/10.1126/science.235.4794.1373 (In English)

Terukov, E. I., Marchenko, A. V., Seregin, P. P. et al. (2018) Parameters of nuclear quadrupole interaction and spatial distribution of electronic defects in $YBa_2Cu_3O_7$ and $La_{2-x}Sr_xCuO_4$ lattices. *Physics of the Solid State*, 60 *(10)*, 1908–1915. https://doi.org/10.1134/S106378341810027X (In English)

Wells, A. F. (1984) *Structural inorganic chemistry*. Oxford: Clarendon Press, 1416 p. (In English)

Wortmann, G., Kolodziejczyk, A., Bergold, M. et al. (1989) Mossbauer studies of $YBa_2Cu_3O_{7-x}$ type high-Tc superconductors. *Hyperfine Interactions*, 50, 555–567. https://doi.org/10.1007/BF02407691 (In English)

Yu, J., Freeman, A. J., Podloucky, R. et al. (1991) Origin of electric-field gradients in high-temperature superconductors: $YBa_2Cu_3O_7$. *Physical Review B*, 43 (1), 532–541. https://doi.org/10.1103/PhysRevB.43.532 (In English)

Yvon, K., Francois, M. (1989) Crystal structure of high-T_c oxides. *Zeitschrift für Physik B*, 76. 413–444. https://doi.org/10.1007/bf01307892 (In English)